bioRxiv (2023)
doi:10.1101/2021.11.27.470201
a Malthusian Relativity paper

$\iota^{**}=7/3\psi$
mrLife.org

On natural selection regulation in the population dynamics of birds and mammals

Lars Witting
Greenland Institute of Natural Resources, Box 570, DK-3900 Nuuk, Greenland. lawi@natur.gl

Abstract Empirical research is increasingly documenting eco-evolutionary dynamics that shape ecological processes. I examine the population dynamic implications of this, analysing whether natural selection improves our ability to predict population dynamic trajectories. Fitting single-species population dynamic models to 3,368 and 480 time-series for 900 species of birds and 208 mammals, I find that selection-based population dynamic models are 320 (se:1.3) times more probable on average than models with no selection. Selection is essential in 76% to 90% of AIC-selected models, explaining 80% of the population dynamics variance, with median selection regulation being 1.5 (se:1.1) times stronger than density regulation. The estimated dynamics is cyclic with median damping ratios for birds and mammals of 0.12 (se:0.0068) and 0.083 (se:0.022), and population periods of 8 (se:0.56) and 6.1 (se:1.1) generations, given stable cycles with damping ratios around zero. These results highlight the necessity of integrating natural selection into population dynamic theory, and they are discussed in relation to the literature resolving several enigmas of population dynamic cycle.

Keywords: Density dependence, eco-evolutionary dynamics, population dynamics, population regulation, timeseries

1 Introduction

Population regulation shapes the dynamics of natural populations, but many population trajectories are not explained by traditional population regulation theory. Take for example the simple case where a population declines gradually until the decline stops and the population begins to increase. This is an often-observed growth pattern, but it is not explained by density-dependent competition. Dependent upon initial conditions, pure density-regulated populations will only increase, or decline, towards carrying capacity showing no change in the direction of growth (over-compensation from strong density regulation does not explain a gradual change in the direction of growth).

For the past century or so, variation in environmental drivers provided the conceptual solution to the lack of fit between single-species population regulation theory and data. These drivers may be density-dependent or independent, including environmental fluctuations and climatic change, as well as predators and prey with theoretically predicted population dynamic cycles. With the dynamics of natural populations correlating with environmental factors (Elton 1924; Koenig 2002; Hu et al. 2021; Herfindal et al. 2022; Jenkins et al. 2022), evidence seems to support the view that population dynamic deviations from monotonic density-regulated growth follow from external factors in most cases. The vast majority of the available timeseries of abundance estimates, however, have no associated data to confirm the extrinsic hypothesis. It is thus often of limited practical use, except as the easy explanation for the lack of fit of deterministic single-species population dynamic models to data.

Delayed density-regulated models are a practical solution when supporting environmental data are missing, providing "single-species" models that explain much of the observed dynamics (e.g., Hutchinson 1948; Witteman et al. 1990; Turchin and Taylor 1992; Hörnfeldt 1994; Hansen et al. 1999a,b; Stenseth et al. 2003). But delayed density-regulated models turn the blind eye to the real problem: the absence of identified but necessary population dynamic interactions. By explicitly not incorporating the mechanisms of the delayed regulation, delayed density regulation is a branch of mathematical engineering that is not part of a formal theory of biology that seeks to explain the observed dynamics from explicitly identified population biological mechanisms.

If we return to studies with a population biological focus, papers on ecologically driven dynamics have advanced by adding stochasticity (Kaitala et al. 1996; McKane and Newman 2005; Yan et al. 2013), environmental oscillations (Post and Forchhammer 2002; Stenseth et al. 2002; Garciá-Comas et al. 2011; Taylor et al. 2013), spatial synchrony (Bjørnstad et al. 1999; Post and Forchhammer 2002; Liebhold et al. 2004; Hansen et al. 2020), demographic details (Murdoch et al. 2002; McCauley et al. 2008; Inchausti and Ginzburg 2009; Miller and Rudolf 2011), and higher-dimensional

interactions (Tyson et al. 2010; Liu et al. 2013; Benincà et al. 2015) to pairwise consumer-resource interactions (reviewed by Myers and Cory 2013; Martínez-Padilla et al. 2014; Barraquand et al. 2017; Krebs et al. 2018; Myers 2018; Oli 2019). But, despite of these efforts, enduring enigmas remain unresolved by the broader population dynamic theory (Myers 2018; Oli 2019; Andreassen et al. 2021).

In a non-cyclic environment, density-regulated populations need trophic interactions for cyclic dynamics in most cases. Yet, by analysing an isolated *Daphnia*-algae system, Murdoch and McCauley (1985) found *Daphnia* to cycle with a relatively fixed period independently of the presence versus absence of a cycle in its prey. Similar paradoxes include snowshoe hares that cycle in the absence of lynx (Keith 1963), and the absence of a firm predator-prey interaction for one of best documented cycles in forest insects (Berryman 1996).

Another issue is the widespread presence of population cycle correlated life history changes that do not follow the expectations of density regulation and predator prey interactions. Where predation affects survival, "most, if not all, cyclic rodent populations are characterised by phase-related changes in body mass, social behaviour, ... and reproductive rates" (Oli 2019). Other lingering problems include that no experimental manipulation of predators and resources "has succeeded in stopping rodent population cycles anywhere" (Oli 2019), and "how can low amplitude cycles persist if high densities are required for the build-up of predators, parasitoids, pathogens or detrimental conditions" (Myers 2018), and why can reproduction remain low across generations in the low phases of cycles where it should be high due to relaxed density regulation?

These issues do not question the general influence of external factors on population dynamics; but they hint at the existence of population dynamic mechanisms that are not sufficiently captured by traditional population dynamic theory. Hence, I take a closer look at the way populations regulate their growth when other things are equal, taking the parsimonious view that to explain the growth patterns of natural populations we need first of all to understand how they regulate their own growth, before we involve external factors.

It has historically been our agreed population regulation concept that sets the stage of our population dynamic investigations. It is, e.g., the monotonic growth of density regulation that has forced biologists to seek external causes to explain the observed trajectories of many species. But population regulation is not restricted to density regulation, as population dynamic feed-back selection is also regulating the growth and abundance of natural populations (Witting 1997, 2000b). From the alternative eco-evolutionary point of view, the lack of fit between traditional single-species population regulation theory and data is not that surprising, as traditional theory assumes that natural selection does not affect population dynamics. With this paper I analyse 3,848 population dynamic timeseries to examine whether natural selection is the missing population regulation component that will make our single species model work as a first approximation to the general population dynamics of birds and mammals.

1.1 On selection regulation

With the Malthusian parameter r being the natural selection fitness of the individual (Fisher 1930), and the average Malthusian parameter being the exponential growth rate of the population (Malthus 1798), the population dynamic growth rate is the trait that is exposed to the strongest natural selection, capturing the natural selection variation in other traits. It is therefore not surprising if natural selection regulates population dynamic growth.

A first attempt to include evolution in population dynamics was based on self-regulation by group-selection (Wynne-Edwards 1962, 1986, 1993), relating to the Chitty (1960) hypothesis. This approach was criticised for unrealistic assumptions (Stenseth 1981, 1995), and I use a different game theoretical analysis focussing on individual selection by density-dependent interactive competition. These selecting interactions generate a population dynamic feed-back that was formulated into a population dynamic model (Witting 1997, 2000a,b), with total regulation from the joint action of density-dependent competition and density-frequency-dependent natural selection.

The regulation that is imposed by this selection accelerates population dynamic growth at abundancies below the naturally selected population dynamic equilibrium, and decelerates growth above, generating cyclic population trajectories that converge on hyperexponential growth at zero abundance (Witting 2000a,b). The predicted population cycles are phase-forgetting being damped in most cases, with amplitudes and cyclic regularities that dependent on the magnitudes and frequencies of external perturbations. This dynamics can replicate the population cycles of forest insects (Witting 1997, 2000b) and the delayed recovery of large whales following commercial exploitation in past centuries (Witting 2013).

Where density regulation suppresses the maximum population dynamic growth rate by density-dependent

competition, selection regulation is the per-generation change in the population dynamic growth rate that follows from the differentiation in the Malthusian parameter across the individuals in the population (see eqns 3 and 6 for details). This differentiation reflects a balance between the interactive quality that individuals use to monopolises resources during density-dependent interactive competition, and the quality-quantity trade-off that selects for a lower quality and an associated increase in the number of offspring produced from given amounts of resources.

The distinction between density regulation and selection regulation is clear on theoretical grounds, but both mechanisms require that the regulating force is sufficiently strongly differentiated across the population densities experienced by natural population. This is expected for natural selection in most animal populations as the feed-back selected population dynamic equilibrium is a selection attractor that explains the evolution of multicellular animals with non-negligible body masses, sexual reproduction, and associated interspecific body mass allometries (Witting 2002, 2008, 2017a,b).

While selection regulation is difficult to prove formally from population dynamic timeseries data, there are many examples of population dynamic responses to natural selection. This evidence includes a two-generation cycle in the abundance and competitive quality of side-blotched lizard (*Uta stansburiana*) in response to selection by density-dependent interactive competition (Sinervo et al. 2000), a selection acceleration of the population dynamic growth rate by up to 40% over few generations (Turcotte et al. 2011a,b), the selection of faster-spreading Covid-19 variants with hyperexponential growth (Baruah 2020; Kupferschmidt 2021; Halley et al. 2021; Pavithran and Sujith 2022), and an increasing number of eco-evolutionary studies documenting evolutionary dynamics on ecological timescales (e.g., Thompson 1998; Law 2000; Sinervo et al. 2000; Hairston et al. 2005; Saccheri and Hanski 2006; Coulson et al. 2011; Schoener 2011; Turcotte et al. 2011; Hendry 2017; Brunner et al. 2019), including evolutionary rescue where selection accelerates the growth rate turning a population decline into increase (Gomulkiewicz and Holt 1995; Agashe 2009; Bell and Gonzalez 2009; Ramsayer et al. 2013; Bell 2017).

The predicted selection change in the population dynamic growth rate follows from an underlying selection of the life history. This includes selection for larger body masses, increased competitive behaviour like aggression, kin groups, and more interacting males at high population densities, and selection for the opposite at low densities (Witting 1997, 2000b). As these phase-related life history changes are one of the enduring enigmas of population cycles, the prediction has already been widely reported from populations with cyclic dynamics, with plenty of literature evidence in favour of selection regulation. This includes a body mass cycle in the *Daphnia* experiments of Murdoch and McCauley (1985), with larger individuals occurring mainly in the late peak phase of a cycle, and smaller individuals mainly in the early increasing phase (Witting 2000b). Similar changes in body mass are widespread in voles and lemmings with cyclic dynamics (Chitty 1952; Hansson 1969; Krebs and Myers 1974; Boonstra and Krebs 1979; Mihok et al. 1985; Lidicker and Ostfeld 1991; Stenseth and Ims 1993; Ergon et al. 2001; Norrdahl and Korpimäki 2002; Lambin et al. 2006), and they have been observed in snowshoe hare (Hodges et al. 1999), cyclic forest insects (Myers 1990; Simchuk et al. 1999), and the highly depleted population of North Atlantic right whales (Stewart et al. 2021).

Population dynamic correlated cycles in other traits have been reported by Naumov et al. (1969) who found that the percentage of males increased in small rodents when densities are high, while females predominate during the low phase. Other cases of an increased male fraction with increased density include white-tailed deer (*Odocoileus virginianus*) (McCullough 1979) and northern elephant seal (*Mirounga angustirostris*) (Le Boeuf and Briggs 1977). Individuals of voles and red grouse (*Lagopus lagopus scotica*) are more aggressive at high than low population densities (Boonstra and Krebs 1979; Stenseth 1982; Watson et al. 1994; Matthiopoulos et al. 2003; Piertney et al. 2008), and the latter have larger kin groups evolving during the increasing phase of a cycle.

To fully anticipate selection regulation it is essential to realise that it reflects the complete response of the population dynamic growth rate to natural selection. This is not restricted to genetic changes, but may include other selection responses from epigenetic inheritance, selected changes in maternal effects and social behaviour, as well as long-term selected phenotypic plasticity in physiological and behavioural traits allowing individuals to respond more directly to cyclic changes in the selection pressure. Cultural inheritance is another factor, where most offspring may balance their quality/quantity investment in their offspring following the balance of their parents, with fewer offspring choosing another balance and thus maintaining the cultural heritable variance of the population. So, if we observe an absence of additive genetic variance, we cannot *a priori* exclude the potential presence of selection reg-

ulation; just as we cannot exclude density regulation when we cannot directly observe the underlying mechanism of the density regulation response.

While it is almost impossible to exclude both density regulation and selection regulation *a priori*, the two mechanisms are clearly separated theoretically, and it is possible to distinguish between them statistically when we analyse a timeseries of abundance estimates. This is because the usual form of density regulation determines the growth rate as a monotonically declining function of density, while population dynamic feed-back selection accelerates and decelerates the growth rate as a function of the density-frequency-dependent selection in the population (Witting 1997, 2000b). This means that the two regulations operate structurally differently on the population dynamics shaping population dynamic trajectories in different ways, and thus the two types of regulation can be estimated statistically when we fit population dynamic models to timeseries of abundance estimates. I will use this ability in this first large-scale comparison where the strength of selection regulation is estimated relatively to that of density regulation for thousands of populations of birds and mammals. It is this level of data analysis that is required to identify if selection regulation is so widespread among natural populations that we need to include it in base-case population dynamic modelling.

2 Method

2.1 Data

To estimate the relative strength of density and selection regulation, I fit population dynamic models to timeseries of abundance estimates. These data are obtained from the Living Planet Index (LPI 2022), the North American Breeding Bird Survey (BBS; Sauer et al. 2017; timeseries compiled by Witting 2023a), the PanEuropean Common Bird Monitoring Scheme (EU; PECBMS 2022), the Netwerk Ecologische Monitoring (NET; Sovon 2022), the Swiss Breeding Bird Index (SWI; Knaus et al. 2022), the British Trust for Ornithology (BTO 2022), the Danish Ornithological Society (DOF 2022), and Svensk Fågeltaxering (SWE; SFT 2022).

Owing to different sources of origin and scales of observation, the timeseries of especially the LPI are of varying quality. The aim of my study is not to explain all these data, but more moderately to estimate the relative importance of density and selection regulation across a large number of timeseries, given models that project the trajectories of the timeseries with a minimum of potential confounding issues. So, to minimise potential side-effects from heterogeneity, I exclude short timeseries and fits with statistical issues, and I select a subset of high-quality data that I analyse separately as a control.

I include only timeseries with more than 10 abundance estimates over at least a 15-year period, resulting in 3,368 timeseries analysed for birds and 480 for mammals, with timeseries scaled for a geometric mean of unity. To avoid confounding effects from incomplete models, they are included for further analysis only if the mean of the residuals are not significantly different from zero ($p < 0.05$ student't), there are no significant autocorrelation in the residuals (lag 1 and 2), no significant correlation between the residuals and the model projection, and the model explains more than 50% of the variance in the data.

Most of the bird timeseries are standardised indices from point-counts, where the overall indices are generated from indices for individual observers on individual routes with a given number of geographically fixed point-counts that are counted in the same way at the same time each year. The calculation of these indices is very standardised, correcting for observer effects and excluding counts performed in bad weather. Thus, given a sufficient number of observers/routes and observations, these bird indices are of high-quality covering a large number of species.

A potential issue with the bird indices is that their geographical coverage may not necessarily represent individual populations. Hence, I restrict my control timeseries to the population dynamics delineated indices (PDDIs) that Witting (2023a) compiled from the raw data of the North American Breeding Bird Survey (Sauer et al. 2017). These are geographically delineated where the spatially synchronised dynamics of different synchronisation optima meet, generating population boundaries with somewhat desynchronised dynamics. These indices are based on the widely confirmed concept of spatially synchronised dynamics (Moran 1953; Stenseth et al. 1998; Ranta et al. 1995; Koenig 1999; Paradis et al. 1999; Haydon et al. 2001; Toms et al. 2005), and they are calculated from more than 6 million bird observations, having yearly abundance estimates for 51 years, covering the geographical range of USA and southern Canada.

For each species, the PDDIs are calculated from up to 105 independent indices covering a $15x7$ longitudinal/latitudinal grid of the whole area. A geographical clustering routine lumps neighbouring indices with synchronised dynamics into larger areas, estimating 462 populations with different dynamics (for method details

see Witting 2023a).

2.2 Population models

I use age-structured models to incorporate the species-specific age-structured delays into the simulated population dynamic trajectories. I parameterise the age-structure at population dynamic equilibrium (denoted by superscript $*$) using the yearly average birth rate (m^*) of mature females, the average age of reproductive maturity (a_m^*), and the yearly survival of offspring (p_0) and individuals older than one year of age (p).

As the age-structure cannot usually be estimated from timeseries of abundance estimates, I obtain the species-specific equilibrium life history parameters from Witting (2023b), and these estimates are kept fixed for each species. While these life history parameters may not necessarily provide the best estimates for all species, they reflect a combination of data and inter-specific extrapolations by allometric correlations across large datasets. Base-case life history models like these are required to construct age structured population dynamic models across a large variety of species.

Having life history estimates for all species, I estimate only the two regulation parameters and some initial conditions from the timeseries of abundance estimates. The stable age-structure at equilibrium is used as an initial age-distribution, and dependent upon the age of reproductive maturity of the species, I may rescale the yearly parameters for 3, 6, or 12 time-steps per year to keep the timesteps of the projection shorter than the age of reproductive maturity.

To find the best single-species model given the age-structure, I develop exponential, hyperexponential, density-regulated, and selection-regulated models for each species. I find the best-fitting-hypothesis by the Akaike information criterion (AIC, Akaike 1973) to trade-off the number of parameters (from 2 to 5) against the likelihood of the four models. This allows me to estimate the relative probability of models with (hyperexponential & selection-regulated) and without (exponential & density-regulated) selection.

The selection-based models are most often statistically preferred over the non-selection models (see result section). Hence, I run a second AIC model-selection to estimate the best selection-regulated models for all populations. In addition to a stable equilibrium, this second selection includes models with a linear trend in equilibrium density. This allows me to quantify not only the relative strengths of regulation by density and selection, but to estimate also if population trends are indicators of underlying changes in the external environment (assuming that a change in equilibrium reflects improved or deteriorating external factors).

The response to regulation by density and selection is set to operate on the birth rate ($m = \tilde{m}/m^*$) and age of reproductive maturity ($a_m = \tilde{a}_m/a_m^*$) by changes in relative parameters ($\tilde{m}$ and $\tilde{a}_m$) that are set to unity at population dynamic equilibrium. As I fit the 1+ component of the population to the abundance data, the estimated regulations on the birth rate include regulation on offspring survival (p_0). Hence, I cover regulation on the three life history parameters that are usually most sensitive to density-dependent changes, although regulation on a_m is allowed only for an extended model-selection analysis of the PDDI timeseries.

The details of the selected-regulated model are described in the supplementary information, with essential differences between the four population models described below.

Exponential growth. This model has constant life history parameters, with the relative birth rate ($\tilde{m}$) and the initial abundance (n_t) being estimated from time-series data.

Hyperexponential growth. In the non-selection models of exponential and density-regulated growth, the vector of the age-structured abundance ($n_{a,t}$) is the only initial condition that is projected in time. In the two selection models there are additional initial conditions that are defined by a vector of competitive quality ($q_{a,t}$). This vector evolves with time, with selection for offspring with increased competitive quality when the abundance is above the equilibrium abundance of the selection-regulated model, selection for no change in quality when the abundance is at the equilibrium, and selection for a decline in offspring quality when the abundance is below the equilibrium.

The age-structured quality of the selection models defines age-structured initial conditions for the relative birth rate

$$\tilde{m}_{a,t} = 1/q_{a,t} \tag{1}$$

and relative reproductive maturity (when included in the selection-regulated model for PDDI timeseries)

$$\tilde{a}_{m,a,t} = q_{a,t} \tag{2}$$

with $q^* = 1$ for all a representing an equilibrium with no growth.

Following the logic of the secondary theorem of natural selection (Robertson 1968; Taylor 1996), the selection induced change in competitive quality—and thus

also in the birth rate and reproductive age—is

$$q_{0,t} = q_t e^{-\gamma_\iota} \tag{3}$$

with average offspring quality (q_0) being a product between the average quality of the mature component

$$q_t = \frac{\sum_{a|a_{m,a,t}\leq a} q_{a,t} n_{a,t}}{\sum_{a|a_{m,a,t}\leq a} n_{a,t}} \tag{4}$$

and a selection response $e^{-\gamma_\iota}$, where

$$\gamma_\iota = -\sigma \, \partial r_i / \partial \ln q_i|_{q_i=q} \tag{5}$$

is the product between the selection gradient ($\partial r_i/\partial \ln q_i|_{q_i=q}$) across the quality variants in the population (denoted by subscript i) and the response ($\sigma \geq 0$) of the population to this force of selection. The response parameter is the additive genetic variance if we focus exclusively on genetic evolution. Yet, as we deal with the complete population response to natural selection, we interpret σ as a more general proportional response of the population per unit selection.

For simplicity briefly consider a discrete model where $r = \ln\lambda \propto \ln m$. Then, when there are no interactive competition and all individuals have equal access to resources, the intra-population variation in the growth rate is $r_i \propto -\ln q_i$ from eqn 1, with a selection gradient of $\partial r_i/\partial \ln q_i|_{q_i=q} = -1$ with $\gamma_\iota = \sigma > 0$. This is the limit case of hyperexponential growth at zero population density. Yet, for the hyperexponential models in this paper, I allow γ_ι to take both positive and negative values to capture the somewhat broader range of options with a constantly accelerating ($\gamma_\iota > 0$) or decelerating ($\gamma_\iota < 0$) growth rate ($\gamma_\iota = 0$ is exponential growth). As the selection gradient on the per-generation growth rate is $-\partial r_i/\partial \ln q_i|_{q_i=q}$ from $r_i \propto -\ln q_i$, the acceleration/deceleration of the growth rate is

$$\dot{r} = dr/dt = \gamma_\iota \tag{6}$$

The intra-population variation and the resulting population response of eqns 5 and 6 represent the underlying mechanisms of natural selection. Yet, it is not necessary to include this modelling of the intra-population variation into the population dynamic equations, and this is because the latter operate from the average response that is captured by eqns 3 and 4.

The hyperexponential model is structurally somewhat more complex than the exponential model, yet it has a single population dynamic parameter only (γ_ι), just as the exponential model has $\tilde{m}$. But, with two initial conditions (n_t & q_t) there are three statistical parameters to fit.

Density-regulated growth. For density-regulated growth I use the Pella and Tomlinson (1969) formulation

$$\tilde{m} = 1 + [\hat{m} - 1][1 - (n/n^*)^\gamma] \tag{7}$$

that has three parameters (the maximum relative birth rate $\hat{m}$, the strength of density regulation γ, and the equilibrium abundance n^*) and one initial condition (n_t) to estimate from timeseries data.

Selection-regulated dynamics. The selection-regulated model includes density regulation

$$\begin{aligned} m_t &= m^* \tilde{m}_t (n^*/n_t)^\gamma \\ a_{m,t} &= a^*_m \tilde{a}_{m,t} (n_t/n^*)^\gamma \end{aligned} \tag{8}$$

formulated as a log-linear deviation from the equilibrium life history, instead of being formulated from a hypothetical maximal growth rate (density regulation on a_m occurs only with a_m selection in the extended analysis of the PDDI timeseries).

The changes in competitive quality—and thus also by eqns 1 and 2 in the intrinsic birth rate and reproductive age—from the population dynamic feedback selection of density-dependent interactive competition, was derived by Witting (1997, 2000b) as

$$q_{0,t} = q_t (n_t/n^*)^{\gamma_\iota} \tag{9}$$

with the selection induced acceleration/deceleration of the growth rate

$$\dot{r} = \gamma_\iota \ln(n^*/n_t) \tag{10}$$

being a log-linear function of the density-dependent ecology.

The selection behind eqns 9 and 10 is based on the biased resource access that emerges when the competitively superior individuals monopolise resources during interactive encounters. This selection is frequency-dependent because the average success of competition for a given variant depends on the average competitive quality across the individuals in the population. The selection is also density-dependent because the average ability to monopolise resources depends on the frequency by which an individual competes against other individuals over resources.

The explicit modelling of the selection requires equations that account for the intra-population variation in competitive quality and resource access (see Witting 1997, 2000b for details). Yet, this selection produces the population level response of eqn 9, which can be incorporated directly into the population dynamic equations, selecting for an increase in average quality when

the abundance is above the equilibrium, and for a decline when the abundance is below.

The population dynamics that follow from the population dynamic feedback selection is cyclic. Thus, I calculate the cycle period (T, in generations) and damping ratio (ζ) to characterise the dynamics. The damping ratio is zero for a stable cycle, and it increases monotonically to a value of unity for the monotonic return of typical density-regulated growth. I calculate the damping ratio

$$\zeta = \frac{1}{\sqrt{1 + 4\pi^2/\delta^2}} \tag{11}$$

by the logarithmic decrement $\delta = \ln(n_{p,1}/n_{p,2})$ of the two successive abundance peaks ($n_{p,1}$ and $n_{p,2}$) that follow from an equilibrium population that is initiated with a positive growth rate where $m_t = 1.5m^*$. The estimated period (T) is the number of generations between these two abundance peaks.

When the γ_ι/γ-ratio is somewhat larger than one the dynamics become unstable with amplitudes that increase over time instead of dampening out. In these cases, I revert $n_{p,1}$ and $n_{p,2}$ in the estimate of $\delta = \ln(n_{p,2}/n_{p,1})$ and multiplies the damping ratio by minus one, so that negative ζ values refer to exploding cycles, with the rate of explosion increasing with a ζ estimate that declines from zero to minus one.

The selection-regulated model has three parameters (γ, γ_ι, & n^*) and two initial conditions (n_t & q_t) to estimate from the data.

2.3 Model fitting & model selection

I use maximum likelihood to estimate the parameters of all models given log normally distributed abundance data

$$\ln L = -\sum_t \frac{[\ln(\tilde{n}_t/n_t)]^2}{2cv_t^2} + \ln cv_t \tag{12}$$

where $\tilde{n}_t$ is the 1+ index estimate in year t, n_t the corresponding model estimate, and $cv_t = \sqrt{\tilde{cv}_t^2 + cv^2}$ the coefficient of variation with $\tilde{cv}_t$ being the coefficient of the index estimate in year t and cv being additional variance that is not captured by the data. The cv parameter is estimated by the likelihood fitting, and it captures among others random variation in the true dynamics of the population and variation in the yearly availability of the population for the yearly census.

To locate the global likelihood maximum of a model given an index trajectory, I projected the model for 100,000 random sets of parameters and initial conditions, applying a Quasi-Newtonian minimiser to the 100 best-fitting random sets. Each of these minimisers located a local likelihood maximum given the initial parameters, and the maximum across the local maxima was selected as the maximum likelihood. To avoid fitting population models with fluctuating or chaotic dynamics to the between-year variation of uncertain abundance estimates, I placed an upper limit of 1.5 on the minimiser estimates of γ and γ_ι.

The maximum likelihood was converted to AIC [$\alpha = 2(k - \ln L)$, k nr. of model parameters], whereafter I applied two rounds of AIC model selection to all timeseries. The first round used the four models from exponential growth to selection-regulated dynamics to determine whether it is essential to include selection into population dynamic models or not. Given the distribution of the AIC-selected models I calculated the fraction of the models that include selection, and the distribution of the probability ratio $p(s/d) = e^{(\alpha_s - \alpha_n)/2}$ of selection (s) versus non-selection models (d), with the s and d models being hyperexponential and exponential growth when one of these were the best AIC-fitting model, and the s and d models being selection-regulated dynamics and density-regulated growth when one of these were the best model.

The second model-selection included five selection-regulated models. In addition to the original model with a stable equilibrium abundance, it included four versions with a linear trend in the population dynamic equilibrium (n^*): *i*) a trend that covered the whole data period (1 extra parameter); *ii*) a trend that started after the first data year (2 extra parameters); *iii*) a trend that ended before the last data year (2 extra parameters); and *iv*) a trend that started after the first year and ended before the last year (3 extra parameters), with a minimum allowed trend period around five years. This last round of model selection was extended with an additional model-selection for the PDDI timeseries, which included the five selected-regulated models with and without additional regulation on the age of reproductive maturity.

For ten populations that experienced an obvious crash the model selection was allowed to include also one year of catastrophic survival. For five populations of large whales, with data obtained from the International Whaling Commission (https://iwc.int), I subtracted annual catches from the simulated trajectories following Witting (2013).

3 Results

A total of 3,368 and 480 timeseries were analysed for 900 and 208 species of birds and mammals, with popu-

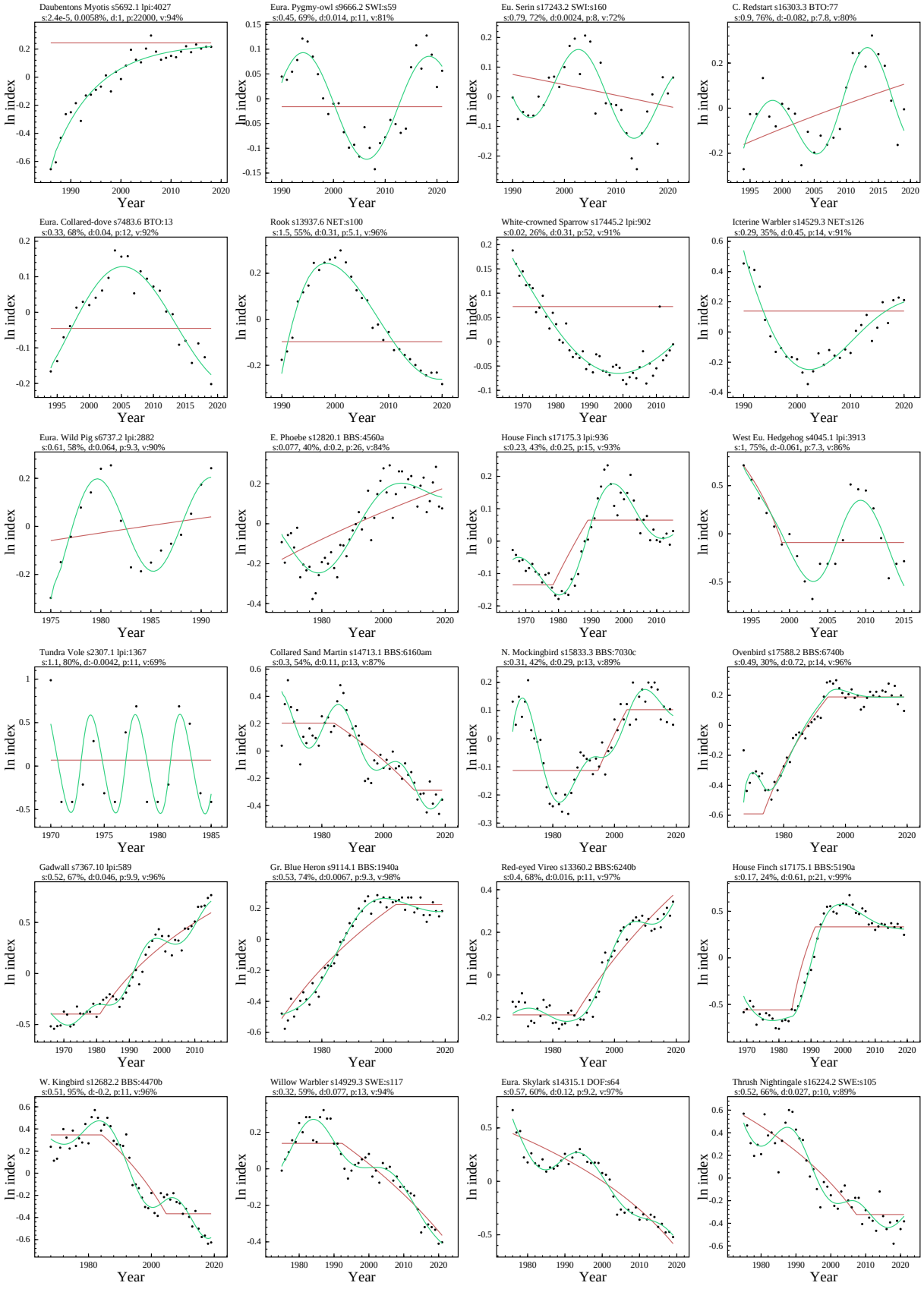

Figure 1: Examples of fits of the selection-regulated model to timeseries of population data. Dots are index series of abundance, red lines the estimated equilibria, green curves the model trajectories, blue curves scaled $n_{t+1} - n_t$ plots (running from blue to red dot), and grey lines the intra-population selection gradients that cause growth acceleration/deceleration. s:γ_ι & $\gamma_\iota/(\gamma_\iota+\gamma)$ in %; d:damping ratio; p:period in generations; v:explained variance.

lation models for 1,953 and 254 bird and mammal populations passing the minimum fitting criterion during the first round of AIC model selection.

For these 2,207 timeseries where a satisfactory model was found, selection-based models were preferred in 76% of the cases (76% for birds & 75% for mammals), with the selection-based models being 320 (se:1.3) times more probable on average (geometric mean) than population dynamic models with no selection included (based on relative AIC). Selection-regulated dynamics were preferred in 36% of the cases, followed by 40% hyperexponential models, 15% exponential, and 8.9% density-regulated models.

The inclusion of selection was more pronounced in the models of the PDDI control timeseries. These included selection in 90% of 251 accepted models, with selection-based models being 43,000 (se:2) times more probable on average than non-selection models. Selection-regulated dynamics were AIC-selected in 60% of the cases, followed by 29% hyperexponential models, 6% exponential, and 4.4% density-regulated models.

With the selection-regulated model allowing for a continuous shift among the three other population dynamic models (exponential when $\gamma = \gamma_\iota = 0$; hyperexponential when $\gamma = 0$ & $\gamma_\iota \neq 0$; density-regulated when $\gamma > 0$ & $\gamma_\iota = 0$), I used the second model-selection between five selection-regulated models to describe the dynamics, allowing for a changes in the equilibrium abundance over time. This resulted in 2,348 and 280 models accepted for birds and mammals, with all models plotted and listed in the Supplementary Information, and some fits to population data shown in Fig. 1.

Most of the estimated trajectories were cyclic around a stable, increasing, or declining equilibrium. This is reflected in the estimated regulation, with median selection regulation (γ_ι) being 0.56 (se:0.011) for birds and 1.2 (se:0.033) for mammals, and median density regulation (γ) being 0.32 (se:0.0093) for birds and 0.44 (se:0.032) for mammals. Fig. 2 shows the distribution of the strength of selection regulation relative to total regulation [i.e., $\gamma_\iota/(\gamma + \gamma_\iota)$] across all timeseries with accepted selection-regulated models. With median estimates of 0.6 (se:0.0058) for birds and 0.66 (se:0.017) for mammals, selection regulation is estimated more important than density regulation in most populations, with median regulation ratios (γ_ι/γ) of 1.5 (se:1.1) and 2 (se:1.3). These results resemble those of the PDDI controls, with relative selection regulation [$\gamma_\iota/(\gamma + \gamma_\iota)$] being 0.58 (se:0.012) at the median across 389 selection-regulated models. Allowing for regulation on reproductive maturity among the PDDI controls, 50% of 400 accepted selection-regulated models were AIC-selected

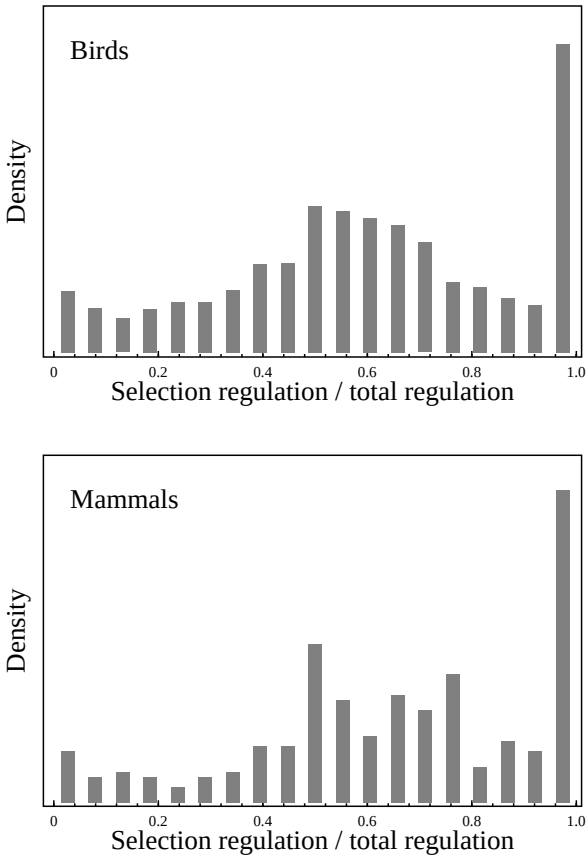

Figure 2: **Selection regulation.** Distributions of point estimates of relative selection regulation ($\gamma_\iota/(\gamma+\gamma_\iota)$) across 2,628 accepted selection-regulated models.

with regulation on both the reproductive rate and age of maturity, having a median relative selection regulation of 0.66 (se:0.015).

The distributions of regulation estimates cover the range from almost pure selection regulation to almost pure density regulation (Fig. 2), but only 5.9% of the bird and 5% of the mammal populations have selection regulation below 10% of total regulation by density and selection. The hypothesis that natural populations of birds and mammals are density-regulated predominantly was not supported.

Where density-regulated growth returns monotonically to the carrying capacity with a damping ratio around unity (as the top left plot in Fig. 1), selection-regulated populations have damped to stable population cycles (Fig. 1), with damping ratios that decline to zero for stable cycles. Some populations may even have exploding cycles with negative damping ratios during smaller time periods, although timeseries with negative

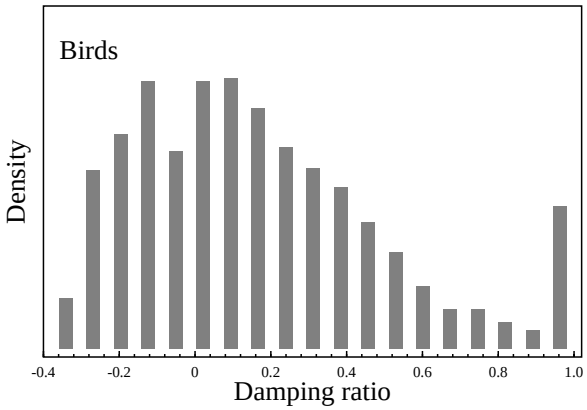

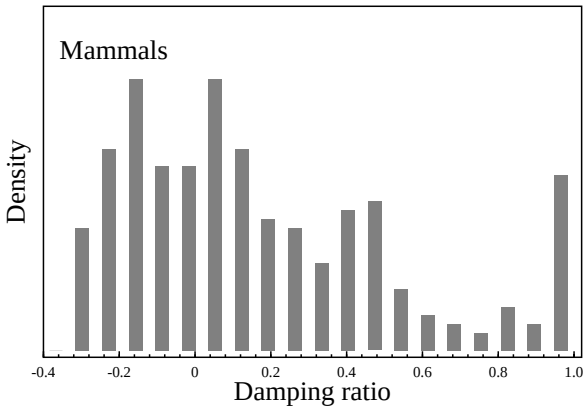

Figure 3: **Damping ratios.** Distributions of point estimates of damping ratios across 2,628 accepted selection-regulated models.

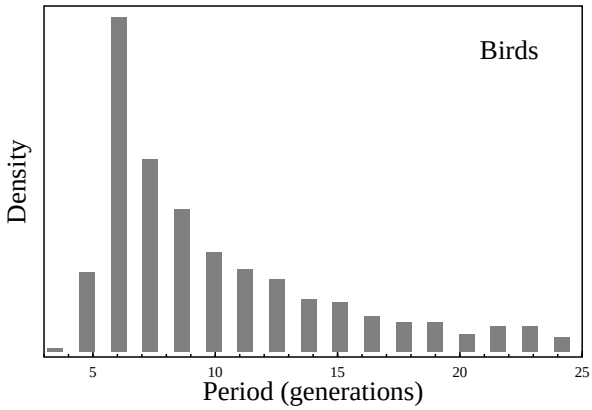

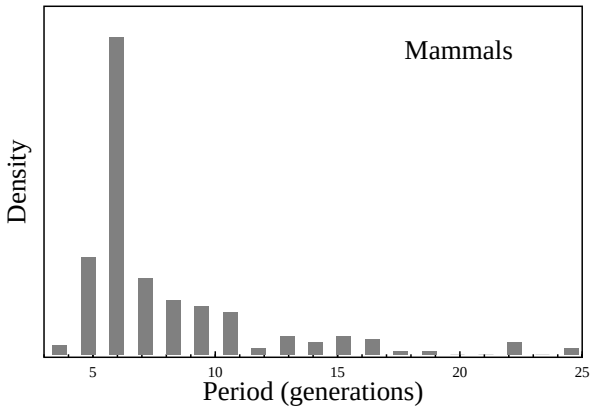

Figure 4: **Population periods.** Distributions of point estimates of the population dynamic cycle period (in generations) across 2,628 accepted selection-regulated models.

damping ratio estimates may reflect uncertainty in our estimation of regulation.

The distributions of the estimated damping ratios are shown in Fig. 3. With median damping ratios around 0.12 (se:0.0068) and 0.083 (se:0.022) the general population dynamics of birds and mammals is best characterised as strongly cyclic. 85% of the bird populations, and 82% of the mammals, have damping ratios that are estimates to be smaller than 0.5. Strongly damped density-regulation-like growth with damping ratios above 0.9 is estimated for 5.4% of the bird populations, and 7.5% of mammals.

The distributions of the periods of the population cycles are shown in Fig. 4. The estimated periods are nearly always above five generations. Although the distributions have long tails toward very long periods, they are highly peaked in the lower range with 53% of all birds, and 71% of all mammals, having periods below 10 generation. Median estimates are 9.4 (se:59) generations for birds and 6.6 (se:180) for mammals, and the period is longer in populations with more damped dynamics. The median period increases from 8 (se:0.56) and 6.1 (se:1.1) generations for birds and mammals with stable dynamics (damping ratios around zero), to 35 (se:8.4) and 25 (se:3.8) for damping ratios around 0.8.

History is unimportant for density-regulated growth in the sense that the current environment and density define the growth rate. But it is essential in selection-regulated dynamics where the initial life history is just as important for current growth as the density-dependent environment. This is the reason for the cyclic dynamics, where the population may remain stable, increase, or decline at the equilibrium abundance dependent upon initial conditions. Where density-regulated populations tend to decline only if the environment deteriorates and the equilibrium abundance declines, selection-regulated populations will often decline about 50% of the time even when the equilibrium

is stable (2nd top plot in Fig. 1), declining (3rd top plot in Fig. 1), or increasing (right top plot in Fig. 1).

Across the accepted models that allow for a trend in equilibrium, the equilibrium abundancies were found to increase for 28% and 18% of the bird and mammal populations, and to decline for 27% and 12%. I we look at intervals where the estimated trajectories are either declining or increasing, we find that 75% of the population dynamic declines were not associated with an estimated decline in the equilibrium abundance, and that 76% of the population dynamic increases were not associated with an equilibrium increase. In fact, 23% of the population declines had increasing equilibria, and 27% of the population increases had declining equilibria. A change in a populations direction of growth is thus not an indicator of a corresponding change in the environment extrinsic to the population, although it may reflect an extrinsic change in some cases.

4 Discussion

With selection-based models being preferred for 76% to 90% of the analysed timeseries, and median selection regulation being 1.5 (se:1.1) times stronger than density regulation, selection regulation is estimated as a necessary component of population dynamic models. Pure density regulation with damping ratios around unity is the exception rather than the rule and unsuited as base-case regulation for birds and mammals. With selection regulation included we have a more elaborate single-species model that describes a very broad range of the observed population dynamic trajectories (see the variety of fits in Fig. 1). These are generally cyclic with median damping ratios around 0.12 (se:0.0068) and 0.083 (se:0.022) for birds and mammals respectively, and population dynamic periods that increase with increased damping, with medians around 8 (se:0.56) and 6.1 (se:1.1) generations for stable cycles with damping ratios around zero.

This selection regulation resolves several enduring enigmas of our theory of population dynamic cycles, extending beyond an alternative mechanism when predator-prey interactions fail. We have already in the introduction seen how selection regulation predicts the widespread—and otherwise unexplained—phase-related changes in the life history traits of species with cyclic population dynamics. And with most of the estimated selection-regulated dynamics being damped phase-forgetting cycles, low amplitude cycles are not a problem because the cyclic dynamics of selection regulation do not depend on high-density amplitudes for the build-up of predators, pathogens, or other detrimental factors.

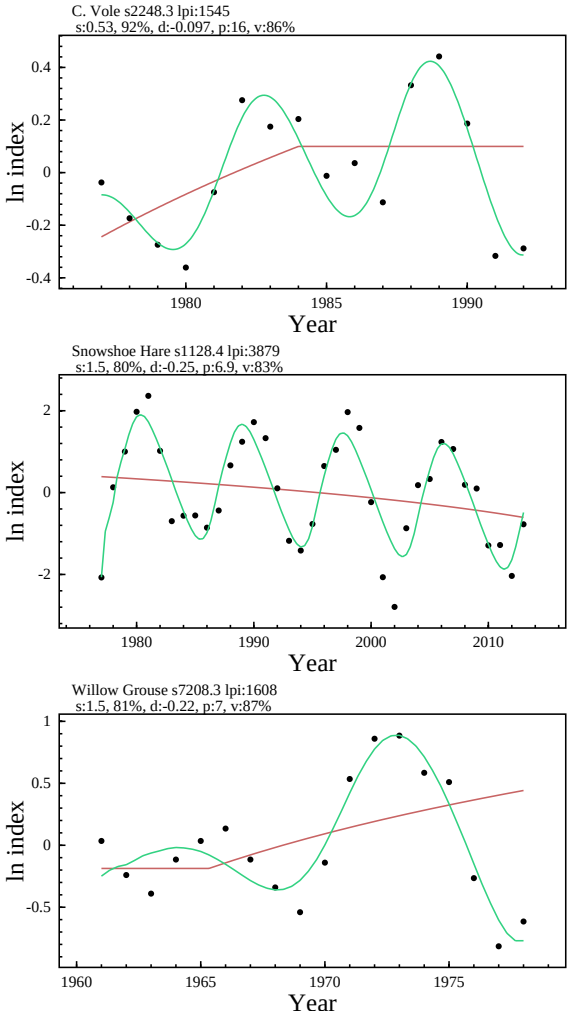

Figure 5: **Population cycles.** Fits of selection-regulated models to abundance estimates of common vole, snowshoe hare, and willow grouse. Data from Krebs et al. (2014), Romankow-Zmudowska and Grala (1994), and Watson et al. (1984). For header details, see Fig. 1

With the damped phase-forgetting dynamics having amplitudes that depend on the magnitude of external perturbations, and persistent cycles that may depend on repeated perturbations, we can expect a diversity of dynamic trajectories across the populations of a given species, dependent upon fluctuations in the external biotic and abiotic environment. Also, with selection regulation accelerating and decelerating the growth rate in smaller steps per generation, there is no longer an issue with a reproductive rate that remains low across several generations at a low population density where density regulation is relaxed. Examples of statistical fits of the

selection-regulated model to the population cycles of common vole (*Microtus arvalis*), snowshoe hare (*Lepus americanus*), and red grouse (*Lagopus lagopus scotica*) are shown in Fig. 5.

Given the widespread evidence in favour of selection regulation, and that it is basically impossible to rule out *a priory*, it is recommended to estimate both density regulation and selection regulation as a base-case when population dynamic models are fitted to data. It should, however, be kept in mind that my results are statistical estimates given the selection-regulated model, and as such they do not exclude other potential reasons for some of the explained variance. While my statistical analyses *i*) lumped random environmental variation beyond the initial conditions of the models into estimates of additional variance in the timeseries of abundance estimates, and *ii*) used linear trends in the equilibrium abundance to capture directional changes in extrinsic factors like habitats, resources and predators, the statistical estimates are not adjusted for secondary effects imposed by e.g. phase-related changes in predation mortality. Thus, should data on per-capita phase-related predation mortality be available it is recommended to include them in model fitting to improve the estimated population dynamic models.

Given that monotonic growth is the exception in birds and mammals, the devil's advocate might argue that the estimated support for selection regulation is nothing but an artefact of rejecting an unrealistically simple density-regulated model. This point however does not provide a suitable alternative, and the conclusion is also too hasty as it does not reflect the details of my study. It is true that a single-species model that includes both density and selection regulation is more elaborate than a model that is regulated by density alone. But it is not given *a priory* that the former model is dynamically more flexible than the latter and thus better suited for the observed dynamics in birds and mammals. Selection regulation could, at least in principle, operate in a similar way as density regulation resulting in equally inflexible models despite of the increased complexity imposed by selection. It is only because regulation by density and selection operates structurally differently on the dynamics that the two components can be distinguished statistically in timeseries of abundance estimates, and it is only because the increased dynamic flexibility is obtained at a low additional parameter cost that the selection-regulated models are preferred over density-regulated models by AIC model selection. We may conclude that the type of population regulation structure that is imposed by natural selection is strongly supported by the population dynamics of birds and mammals.

Delayed density-regulated models have a similar statistical advantage, but they are usually not testing explicit biological hypotheses. A delayed regulation from explicitly identified inter-specific interactions, e.g., should instead be accounted for by mechanistic models that are structured to incorporate the delays of the age-structured life histories of the interacting species. This, however, will typically require the addition of several extra parameters, and inter-specific explanations are thus typically less parsimonious than selection-regulated explanations (which have the same number of parameters and one extra initial condition to fit, relative to density-regulated models).

Almost perfect fits of theoretical population trajectories to data may always be obtained by adding timestep specific environmental perturbations to simple models. But this will normally require many extra time-specific conditions/parameters to fit per timeseries, and these methods are then even less statistically supported. In the end, when constructing a dynamic model for a population, the parsimonious way is to analyse if the population regulation of the population will explain the dynamics of that population. The model may then be extended secondarily with explicit inter-specific interactions to fine-tune the estimate or seek alternative explanations should density and selection regulation fail to explain the dynamics.

Another advantage of incorporating natural selection relates to animal abundance. Where traditional non-selection population dynamic theory struggles to explain the abundance of animals (May 2020), population dynamic feed-back selection explains much of the observed inter-specific variation in the abundance of birds and mammals, given as a function of the naturally selected body mass with superimposed inter-specific competition (Witting 2023). It appears that the density-frequency-dependent feed-back selection of interactive competition is essential to progress our understanding of the dynamics and densities of natural populations.

Acknowledgements

I thank all who collect and publish population data, and reviewers for comments. The selection-regulated models are available for online simulations at https://mrLife.org.

Supplementary Information

si-appendix Model appendix

si-plot Population plots

si-model Population models

References

Agashe D. (2009). The stabilizing effect of intraspecific genetic variation on population dynamics in novel and ancestral habitats. Am. Nat. 174:255–267.

Akaike H. (1973). Information theory as an extension of the maximum likelihood principle. In: Petrov B. N. Csaki F. (eds). Second International Symposium on Information Theory: Akademiai Kiado, pp 267–281.

Andreassen H. P., Sundell J., Ecke F., Halle S., Haapakoski M., Henttonen H., Huitu O., Jacob J., Johnsen K., Koskela E., Luque-Larena J. J., Lecomte N., Leirs H., Marien J., Neby M., Ratti O., Sievert T., Singleton G. R., Cann J. v., Broecke B. V., Ylonen H. (2021). Population cycles and outbreaks of small rodents: ten essential questions we still need to solve. Oecologia 195:601–622.

Barraquand F., Louca S., Abbott K. C., Cobbold C. A., Cordoleani F., DeAngelis D. L., Elderd B. D., Fox J. W., Greenwood P., Hilker F. M., Murray D. L., Stieha C. R., Taylor R. a., Vitense K., Wolkowicz G. S. K., Tyson R. C. (2017). Moving forward in circles: challenges and opportunities in modelling population cycles. Ecol. Lett. 20:1074–1092.

Baruah H. K. (2020). Hyper-exponential growth of COVID-19 during resurgence of disease in Russia. Preprint at medRxiv https://dx.doi.org/10.1101/2020.10.26.20219626.

Bell G. (2017). Evolutionary rescue. Ann. Rev. Ecol. Evol. Syst. 48:605–627.

Bell G. Gonzalez A. (2009). Evolutionary rescue can prevent extinction following enviromental change. Ecol. Lett. 12:942–948.

Benincà E., Ballantine B., Ellner S. P., Huisman J. (2015). Species fluctuations sustained by a cyclic succession at the edge of chaos. Proc. Nat. Acad. Sci. 112:6389–6394.

Berryman A. A. (1996). What causes population cycles of forest lepidoptera? Trends Ecol. Evol. 11:28–32.

Bjørnstad O. N., Ims R. A., Lambin X. (1999). Spatial population dynamics: analyzing patterns and processes of population synchrony. Trends Ecol. Evol. 14:427–432.

Boonstra R. Krebs C. J. (1979). Viability of large- and small-sized adults in fluctuating vole populations. Ecology 60:567–573.

Brunner F. S., Deere J. A., Egas M., Eizaguirre C., Raeymaekers J. A. M. (2019). The diversity of eco-evolutionary dynamics: Comparing the feedbacks between ecology and evolution across scales. Funct. Ecol. 33:7–12.

BTO (2022). British Trust for Ornithology. Population trend graphs. https://www.bto.org.

Chitty D. (1952). Mortality among voles (*Microtus agrestis*) at Lake Vyrnwy, Montgomeryshire in 1936-9. Phil. Trans. R. Soc. Lond. 236:505–552.

Chitty D. (1960). Population processes in the voles and their relevance to general theory. Can. J. Zool. 38:99–113.

Coulson T., Macnulty D. R., Stahler D. R., Vonholdt B., Wayne R. K., Smith D. W. (2011). Modeling Effects of Environmental Change on Wolf Population Dynamics, Trait Evolution, and Life History. Science 334:1275–1278.

DOF (2022). Dansk Ornitologisk Forening. Punkttællinger. https://www.dof.dk.

Elton C. S. (1924). Periodic fluctuations in number of animals: their causes and effects. Brit. J. Exp. Biolo. 2:119–163.

Ergon T., Lambin X., Stenseth N. C. (2001). Life-history traits of voles in a fluctuating population respond to the immediate environment. Nature 411:1043–1045.

Fisher R. A. (1930). The genetical theory of natural selection. Clarendon, Oxford.

Garcia-Comas C., Stemmann L., Ibanez F., Berline L., Mazzocchi M., Gasparini S., Picheral M., Gorsky G. (2011). Zooplankton long-term changes in the Northwest Mediterranean Sea: decadal periodicity forced by winter hydrographic conditions related to large-scale atmospheric changes? J. Mar. Syst. 87:216–226.

Gomulkiewicz R. Holt R. D. (1995). When does evolution by natural selection prevent extinction? Evolution 49:201–207.

Hairston N. G. J., Ellner S. P., Geber M. A., Yoshida T., Fox J. A. (2005). Rapid evolution and the convergence of ecological and evolutionary time. Ecol. Lett. 8:1114–1127.

Halley J. M., Vokou D., Pappas G., Sainis I. (2021). SARS-CoV-2 mutational cascades and the risk of hyper-exponential growth. Microbial Pathigenesis 161:https://doi.org/10.1016/j.micpath.2021.105237.

Hansen B. B., Grøtan V., Herfindal I., Lee A. M. (2020). The Moran effect revisited: spatial population synchrony under global warming. Ecography 43:1591–1602.

Hansen T. F., Stenseth N. C., , Henttonen H. (1999a). Multiannual vole cycles and population regulation during long winters: an analysis of seasonal density fependence. Am. Nat. 154:129–139.

Hansen T. F., Stenseth N. C., Henttonen H., Tast J. (1999b). Interspecific and intraspecific competition as causes of direct and delayed density dependence in a fluctuating vole population. Proc. Nat. Acad. Sci. USA 96:986–991.

Hansson L. (1969). Spring populations of small mammals in central Swedish Lapland in 1964-1968. Oikos 20:431–450.

Haydon D. T., Stenseth N. C., Boyce M. S., Greenwood P. E. (2001). Phase coupling and synchrony in the

spatiotemporal dynamics of muskrat and mink populations across Canada. Proc. Nat. Acad. Sci. 98:13149–13154.

Hendry A. P. (2017). Eco-evolutionary dynamics. Princeton University Press, Princeton.

Herfindal I., Lee A. M., Marquez J. F., Moullec M. L., Peeters B., Hansen B. B., Henden J., Sæther B. (2022). Environmental effects on spatial population dynamics and synchrony: lessons from northern ecosystems. Clim. Res. 86:113–123.

Hodges K. E., Stefan C. I., Gillis E. A. (1999). Does body condition affect fecundity in a cyclic population of snowshoe hares? Can. J. Zool. 77:1–6.

Hörnfeldt B. (1994). Delayed density dependence as a determinant of vole cycles. Ecology 73:791–806.

Hu G., Stefanescu C., Oliver T. H., Roy D. B., Brereton T., Swaay C. V., Reynolds D. R., Chapman J. W. (2021). Environmental drivers of annual population fluctuations in a trans-Saharan insect migrant. Proc. Nat. Acad. Sci. 118:e2102762118.

Hutchinson G. E. (1948). Circular causal systems in ecology. Ann. N.Y. Acad. Sci. 50:221–246.

Inchausti P. Ginzburg L. R. (2009). Maternal effects mechanism of population cycling: a formidable competitor to the traditional predator. Phil. Trans. R. Soc. B: Biol. Sci 364:1117–1124.

Jenkins G. P., Coleman R. A., Barrow J. S., Morrongiello J. R. (2022). Environmental drivers of fish population dynamics in an estuarine ecosystem of south-eastern Australia. Fish. Manag. Ecol. 29:693–707.

Kaitala V., Ranta E., Lindstrom J. (1996). Cyclic population dynamics and random perturbations. J. Anim. Ecol. 65:249–251.

Keith L. B. (1963). Wildlife's ten year cycle. University of Wisconsin Press, Madison.

Knaus P., Schmid H., Strebel N., Sattler T. (2022). The State of Birds in Switzerland 2022 online. http://www.vogelwarte.ch.

Koenig W. D. (1999). Spatial autocorrelation of ecological phenomena. Trends Ecol. Evol. 14:22–26.

Koenig W. D. (2002). Global patterns of environmental synchrony and the Moran effect. Ecography 25:283–288.

Krebs C. J., Boonstra R., Boutin S. (2018). Using experimentation to understand the 10-year snowshoe hare cyele in the boreal forest of North America. J. Anim. Ecol. 87:87–100.

Krebs C. J., Boonstra R., Boutin S., Sinclair A. R. E., Smith J. M. M., Gilbert B. S., Martin K., O'Donoghue M., Turkington R. (2014). Trophic dynamics of the boreal forest of the Kluane region. Arctic 67:71–81.

Krebs C. J. Myers J. (1974). Population cycles in small mammals. Ad. Ecol. Res. 8:267–399.

Kupferschmidt K. (2021). Fast-spreading U.K. virus variant raises alarm. Science 371:9–10.

Lambin X., Bretagnolle V., Yoccoz N. G. (2006). Vole population cycles in northern and southern Europe: Is there a need for different explanations for single pattern? J. Anim. Ecol. 75:340–349.

Law R. (2000). Fishing, selection, and phenotypic evolution. ICES J. Marine Sci. 57:659–668.

Le Boeuf B. J. Briggs K. T. (1977). The cost of living in a seal harem. Mammalia 41:167–195.

Lidicker W. Z. Ostfeld R. S. (1991). Extra-large body size in California voles: Causes and fitness consequences. Oikos 61:108–121.

Liebhold A., Koenig W. D., Bjørnstad O. N. (2004). Spatial synchrony in population dynamics. Ann. Rev. Ecol. Evol. Syst. 35:467–490.

Liu R., Gourley S. A., DeAngelis D. L., Bryant J. P. (2013). A mathematical model of woody plant chemical defenses and snowshoe hare feeding behavior in boreal forests: the effect of age-dependent toxicity of twig segments. SIAM J. Appl. Math. 73:281–304.

LPI (2022). Living Planet Index database. www.livingplanetindex.org.

Malthus T. R. (1798). An essay on the principle of population. Johnson, London.

Martinez-Padilla J., Redpath S. M., Zeineddine M., Mougeot F. (2014). Insights into population ecology from long-term studies of red grouse *Lagopus lagopus scoticus*. J. Anim. Ecol. 83:85–98.

Matthiopoulos J., Moss R., Mougeot F., Lambin X., Redpath S. M. (2003). Territorial behaviour and population dynamics in red grouse *Lagopus lagopus scoticus*. II. Population models. J. Anim. Ecol. 72:1083–1096.

May R. M. (2020). What determines population density?. In: Dobson A., Holt R. D., Tilman D. (eds). Unsolved problems in ecology: Princeton University Press, Princeton, pp 67–75.

McCauley E., Nelson W., Nisbet R. (2008). Small-amplitude cycles emerge from stage-structured interactions in daphniaalgal systems. Nature 455:1240–1243.

McCullough D. R. (1979). The George River Deer Herd: Population ecology of a k-selected species. Univ. Michigan Press, Ann Arbor.

McKane A. J. Newman T. J. (2005). Predator-prey cycles from resonant amplification of demographic stochasticity. Phys. Rev. Lett. 94:218102.

Mihok S., Turner B. N., Iverson S. L. (1985). The characterization of vole population dynamics. Ecol. Monogr. 55:399–420.

Miller T. Rudolf V. (2011). Thinking inside the box: communitylevel consequences of stage-structured populations. Trends Ecol. Evol. 26:457–466.

Moran P. A. P. (1953). The statistical analysis of the canadian lynx cycle. Aust. J. Zool. 1:163–173.

Murdoch W. W., Kendall B. E., Nisbet R. M., Briggs C. J., Mccauley E., Bolser R. (2002). Single-species models for many-species food webs. Nature 417:541–543.

Murdoch W. W. McCauley E. (1985). Three distinct types of dynamic behavior shown by a single planktonic system. Nature 316:628–630.

Myers J. H. (1990). Population cycles of western tent caterpillars: experimental introductions and synchrony of fluctuations. Ecology 71:986–995.

Myers J. H. (2018). Population cycles: generalities, exceptions and remaining mysteries. Proc. R. Soc. B. 285:20172841.

Myers J. H. Cory J. S. (2013). Population cycles in forest Lepidoptera revisited. Ann. Rev. Ecol. Evol. Syst. 44:565–592.

Naumov S. P., Gibet L. A., Shatalova S. (1969). Dynamics of sex ratio in respect to changes in numbers of mammals. Zh. Obshch. Biol. 30:673–680.

Norrdahl K. Korpimäki E. (2002). Changes in individual quality during a 3-year population cycle of voles. Oecologia 130:239–249.

Oli M. K. (2019). Population cycles in voles and lemmings: state of the science and future directions. Mamm. Rev. 49:226–239.

Paradis E., Baillie S. R., Sutherland W. J., Gregory R. D. (1999). Dispersal and spatial scale affect synchrony in spatial population dynamics. Ecol. Lett. 2:114–120.

Pavithran I. Sujith R. I. (2022). Extreme COVID-19 waves reveal hyperexponential growth and finite-time singularity. Chaos 32:041104.

PECBMS (2022). Pan-European Common Bird Monitoring Scheme. https://pecbms.info.

Pella J. Tomlinson P. (1969). A generalized stock production model. Trop. Tuna. Comm. Bull. 13:419–496.

Piertney S. B., Lambin X., Maccoll A. D. C., Lock K., Bacon P. J., Dallas J. F., Leckie F., Mougeot F., Racey P. A., Redpath S., Moss R. (2008). Temporal changes in kin structure through a population cycle in a territorial bird, the red grouse *Lagopus lagopus scoticus*. Mol. Ecol. 17:2544–2551.

Post E. Forchhammer M. C. (2002). Synchronization of animal population dynamics by large-scale climate. Nature 420:168–171.

Ramsayer J., Kaltz O., Hochberg M. E. (2013). Evolutionary rescue in populations of *Peudomonas fluoresens* across an antibiotic gradient. Evol. Appl. 6:608–616.

Ranta E., Kaitala V., Lindstrom J., Linden H. (1995). Synchrony in population dynamics. Proc. R. Soc. Lond. B. 262:113–118.

Robertson A. (1968). The spectrum of genetic variation. In: Lewontin R. C. (ed). Population Biology and Evolution: Syracuse University Press, New York, pp 5–16.

Romankow-Zmudowska A. Grala B. (1994). Occurrence and distribution of the common vole, Microtus arvalis [Pallas], in legumes and seed grasses in Poland between 1977 and 1992. Polish Ecol. Stu. 20:503–508.

Saccheri I. Hanski I. (2006). Natural selection and population dynamics. Trends Ecol. Evol. 21:341–347.

Sauer J. R., Niven D. K., Hines J. E., Ziolkowski D. J., Pardieck K. L., Fallon J. E., Link W. A. (2017). The North American Breeding Bird Survey, Results and analysis 1996 – 2015. Version 2.07.2017. USGS Patuxent Wildlife Research Center, Laurel, Maryland, Available at www.mbr-pwrc.usgs.gov/bbs/bbs.html.

Schoener T. W. (2011). The newest synthesis: understanding the interplay of evolutionary and ecological dynamics. Science 331:426–429.

SFT (2022). Svensk Fågeltaxering. http://www.fageltaxering.lu.se.

Simchuk A. P., Ivashov A. V., Companiytsev V. A. (1999). Genetic patters as possible factors causing population cycles in oak leafroller moth, *Tortrix viridana* L. For. Ecol. Manage. 113:35–49.

Sinervo B., Svensson E., Comendant T. (2000). Density cycles and an offspring quantity and quality game driven by natural selection. Nature 406:985–988.

Sovon (2022). Netwerk Ecologische Monitoring, Sovon. Provincies & CBS. http://sovon.nl.

Stenseth N. C. (1981). On chitty's theory for fluctuating population: the importance of genetic polymorphism in the generation of regular density cycles. J. theor. Biol. 90:9–36.

Stenseth N. C. (1982). Causes and consequences of dispersal in small mammals. In: Swingland I. Greenwood P. (eds). The ecology of animal movement: Oxford University Press, Oxford, pp 62–101.

Stenseth N. C. (1995). Snowshoe hare populations: Squeezed from below and above. Science 269:1061–1062.

Stenseth N. C., Falck W., Chan K.-S., Bjørnstad O. N., O'Donoghue M., Tong H., Boonstra R., Boutin S., Krebs C. J., Yoccoz N. G. (1998). From patterns to processes: Phase and density dependencies in the Canadian lynx cycle. Proc. Nat. Acad. Sci. USA 26:15430–15435.

Stenseth, N. C. & Ims, R., eds (1993). The biology of lemmings. Academic Press, San Diego.

Stenseth N. C., Mysterud A., Ottersen G., Hurrell J. W., Chan K. S., Lima M. (2002). Ecological effects of climate fluctuations. Science 297:1292–1296.

Stenseth N. C., Viljugrein H., Saitoh T., Hansen T. F., Kittilsen M. O., Bølviken E., Glöckner F. (2003). Seasonality, density dependence, and population cycles in Hokkaido voles. Proc. Nat. Acad. Sci. 100:11478–11483.

Stewart J. D., Durban J. W., Knowlton A. R., Lynn M. S., Fearnbach H., Barbaro J., Perryman W. L., Miller C. A., Moore M. J. (2021). Decreasing body lengthts in North Atlantic right whales. Curr. Biol. 31:1–6.

Taylor P. D. (1996). The selection differential in quantitative genetics and ess models. Evolution 50:2106–2110.

Taylor R. A., White A., Sherratt J. (2013). How do variations in seasonality affect population cycles? Proc. R.

Soc. Lond. B. https://doi.org/10.1098/rspb.2012.2714.
Thompson J. N. (1998). Rapid evolution as an ecological process. Trends Ecol. Evol. 13:329–332.
Toms J. D., Hannon S. J., Schmiegelow F. K. A. (2005). Population dynamics of songbirds in the boreal mixedwood forests of Alberta, Canada: Estimating minimum and maximum extents of spatial population synchrony. Land. Ecol. 20:543–553.
Turchin P. Taylor A. D. (1992). Complex dynamics in ecological time series. Ecology 73:289–305.
Turcotte M. M., Reznick D. N., Hare J. D. (2011a). The impact of rapid evolution on population dynamics in the wild: experimental test of eco-evolutionary dynamics. Ecol. Lett. 14:1084–1092.
Turcotte M. M., Reznick D. N., Hare J. D. (2011b). Experimental assessment of the impact of rapid evolution on population dynamics. Evol. Ecol. Res. 13:113–131.
Tyson R., Haines S., Hodges K. (2010). Modelling the Canada lynx and snowshoe hare population cycle: the role of specialist predators. Theor. Ecol. 3:97–111.
Watson A., Moss R., Parr R., Mountford M. D., Rothery P. (1994). Kin landownership, differential aggression between kin and non-kin, and population fluctuations in red grouse. J. Anim. Ecol. 63:39–50.
Watson A., Moss R., Rothery P., Parr R. (1984). Demographic causes and predictive models of population fluctuations in red grouse. J. Anim. Ecol. 53:639–662.
Witteman G. J., Redfearn A., Pimm S. L. (1990). The extent of complex population changes in nature. Evol. Ecol. 4:173–183.
Witting L. (1995). The body mass allometries as evolutionarily determined by the foraging of mobile organisms. J. theor. Biol. 177:129–137, https://doi.org/10.1006/jtbi.1995.0231.
Witting L. (1997). A general theory of evolution. By means of selection by density dependent competitive interactions. Peregrine Publisher, Århus, 330 pp, URL https://mrLife.org.
Witting L. (2000a). Interference competition set limits to the fundamental theorem of natural selection. Acta Biotheor. 48:107–120, https://doi.org/10.1023/A:1002788313345.
Witting L. (2000b). Population cycles caused by selection by density dependent competitive interactions. Bull. Math. Biol. 62:1109–1136, https://doi.org/10.1006/bulm.2000.0200.
Witting L. (2002). From asexual to eusocial reproduction by multilevel selection by density dependent competitive interactions. Theor. Pop. Biol. 61:171–195, https://doi.org/10.1006/tpbi.2001.1561.
Witting L. (2008). Inevitable evolution: back to *The Origin* and beyond the 20th Century paradigm of contingent evolution by historical natural selection. Biol. Rev. 83:259–294, https://doi.org/10.1111/j.1469–185X.2008.00043.x.
Witting L. (2013). Selection-delayed population dynamics in baleen whales and beyond. Pop. Ecol. 55:377–401, https://dx.doi.org/10.1007/s10144–013–0370–9.
Witting L. (2017a). The natural selection of metabolism and mass selects allometric transitions from prokaryotes to mammals. Theor. Pop. Biol. 117:23–42, https://dx.doi.org/10.1016/j.tpb.2017.08.005.
Witting L. (2017b). The natural selection of metabolism and mass selects lifeforms from viruses to multicellular animals. Ecol. Evol. 7:9098–9118, https://dx.doi.org/10.1002/ece3.3432.
Witting L. (2023a). On the natural selection of body mass allometries. Acta Oecol. 118:103889, https//dx.doi.org/10.1016/j.actao.2023.103889.
Witting L. (2023b). Population dynamic population delineation in North American birds. Preprint at bioRxiv https://dx.doi.org/10.1101/2023.08.29.555290.
Witting L. (2023c). The population dynamic life histories of the birds and mammals of the world. Preprint at bioRxiv https://dx.doi.org/10.1101/2021.11.27.470200.
Wynne-Edwards V. C. (1962). Animal dispersion in relation to social behavior. Oliver & Boyd, Edinburgh.
Wynne-Edwards V. C. (1986). Evolution through group selection. Blackwell Scientific Publications, Oxford.
Wynne-Edwards V. C. (1993). A rationale for group selection. J. theor. Biol. 162:1–22.
Yan C., Stenseth N. C., Krebs C. J., Zhang Z. (2013). Linking climate change to population cycles of hares and lynx. Global Change Biol. 19:3263–3271.

5 Model appendix

The age-structure of each model is determined from three species specific parameters obtained from Witting (2023a). These are the age of reproductive maturity (first reproductive event) in years ($\acute{a}_m$), the annual rate of reproduction at population dynamic equilibrium ($\acute{m}^*$), and the annual survival ($\acute{p}$) of mature individuals. These parameters were converted to the appropriate timescale, with $a_m = \acute{a}_m/\Delta t$, $m^* = \acute{m}^*\Delta t$, $p = \acute{p}^{1/\Delta t}$, and $\Delta t \leq \min(1, \acute{a_m})$ being the timestep of the simulation model in years.

Having estimates of the three parameters on the timescale of the model, p was used as the survival rate for all age-classes except age-class zero. To calculate age-class zero survival, I converted adult survival into the reproductive period $t_r = 1/(1-p)$, to calculate lifetime reproduction $R = t_r m^*$, and $l_m = 2/R$ from the population dynamic equilibrium constraint $l_m R/2 = 1$, with l_m being the probability that a new-born survives to a_m. Then, having l_m, age class zero survival was calculated as $p_0 = l_m p^{1-a_m}$.

With $x \gg a_m$ being the maximum lumped age-class, the number $n_{a,t}$ of individuals of age $0 < a < x$ at timestep t is

$$n_{a,t} = p_{a-1} n_{a-1,t-1} \tag{13}$$

and the number in age-class x

$$n_{x,t} = p_x n_{x,t-1} + p_{x-1} n_{x-1,t-1} \tag{14}$$

with $p_a = p_0$ for $a = 0$ and $p_a = p$ for $a \geq 1$. Let the number of individuals in each age-class relate to time just after each timestep transition, with offspring at t being produced by the $t-1$ individuals that survive to the $t-1 \rightarrow t$ transition, with the density dependent ecology being approximated by the average 1+ abundance of the two timesteps:

$$\hat{n}_t = 0.5 \sum_{a \geq 1} n_{a,t} + n_{a,t-1}. \tag{15}$$

Together with the quality-quantity trade-off, the competitive qualities of the individuals define their relative birth rate

$$\tilde{m}_{a,t} = 1/q_{a,t} \tag{16}$$

as well as their relative age of reproductive maturity

$$\tilde{a}_{m,a,t} = q_{a,t} \tag{17}$$

with the population dynamic equilibrium having $q^* = 1$ for all a. More generally $q_{a,t} = q_{a-1,t-1}$ and

$$q_{x,t} = \frac{q_{x,t-1} p_x n_{x,t-1} + q_{x-1,t-1} p_{x-1} n_{x-1,t-1}}{n_{x,t}} \tag{18}$$

assuming that there is no change in the quality of a cohort over time. The quality of offspring

$$q_{0,t} = \frac{\sum_{a|a_{m,a,t} \leq a} q_{a,t} n_{a,t}}{\sum_{a|a_{m,a,t} \leq a} n_{a,t}} \left(\frac{\hat{n}_t}{\hat{n}^*} \right)^{\gamma_\iota} \tag{19}$$

is the average quality of the mature component multiplied by the density dependent selection, with γ_ι being the selection response.

Density regulation

$$\begin{aligned} m_{a,t} &= m^* \tilde{m}_{a,t} (\hat{n}^*/\hat{n}_t)^\gamma \\ a_{m,a,t} &= a^*_m \tilde{a}_{m,a,t} (\hat{n}_t/\hat{n}^*)^\gamma \end{aligned} \tag{20}$$

is formulated as a log-linear deviation from the equilibrium life history, with γ being the strength of regulation, and the number of offspring in age-class zero being

$$n_{0,t} = 0.5 \sum_{a|a_{m,a,t} \leq a} m_{a,t} n_{a,t}. \tag{21}$$

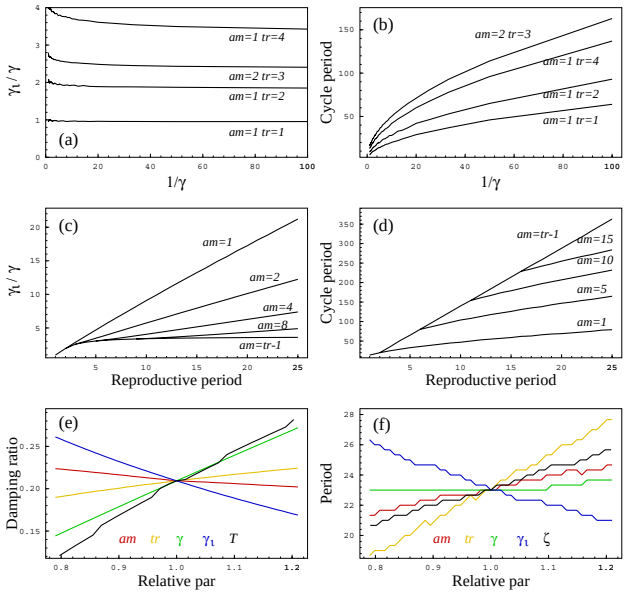

Figure 6: **Dynamic behaviour. Plot a to d:** The γ_ι/γ-ratio, and period (in years), of a stable population cycle ($\zeta = 0$) as a function of $1/\gamma$ (plot **a** and **b**) and the reproductive period (plot **c** and **d** for $\gamma = 0.2$), for different combinations of tm and tr. **Plot e and f:** The damping ratio (ζ) and population period (T) as a function of the parameters $x \in \{am, tr, \gamma, \gamma_\iota, \zeta, T\}$, relative ($x/\hat{x}$) to $\hat{x} \in \{am = 1, tr = 2.8, \gamma = 0.51, \gamma_\iota = 0.76, \zeta = 0.21, T = 23\}$. The dependence on T in plot **e**, and on ζ in plot **f**, is given by their responses to changes in γ_ι.

The initial conditions of an iteration are the same quality across all individuals and the initial abundance with a stable age-structure

$$c_a = l_a / \sum_{a \geq 0} l_a \tag{22}$$

where $l_0 = 1$, $l_a = p_0\ p^{a-1}$ for $1 \leq a < x$, and $l_x = p_0\ p^{x-1}/(1-p)$.

The population dynamic behaviour of a discrete version of the selection-regulated model was described by Witting (1997, 2000b). This model has damped population cycles when $\gamma_\iota < \gamma$, neutrally stable cycles when $\gamma_\iota = \gamma$, and repelling cycles when $\gamma_\iota > \gamma$. The population period of the stable cycles increases from four to an infinite number of generations as the $\gamma_\iota = \gamma$ parameters decline from two to zero. For a given γ the period increases with a decline in γ_ι, i.e., with an increasingly damped cycle. When, for a stable cycle, $\gamma_\iota = \gamma$ increases from two to four, there is an extra period in the amplitude of the population period, with the latter declining monotonically to two generations, with the

dynamics becoming chaotic when $\gamma_\iota = \gamma$ increases beyond four.

The age-structured model with overlapping generations behave in a similar way, but the dynamics depend on the age of reproductive maturity (a_m) and the reproductive period [$t_r = 1/(1-p)$]. The age-structured model converges on the discrete model as $a_m \to 1$, $t_r \to 1$, and $p \to 0$. With no regulation on maturity, the period (T) of the stable population cycle remains a declining function of γ (Fig. 6b), with the slope/exponent (β) of the $\ln T \propto \beta \ln \gamma$ relation being -0.5 (estimated by linear regression). The cyclic dynamics become more and more stable with a decline in γ_ι, but the damping is also dependent on a_m and t_r. The stable cycle, e.g., has a γ_ι/γ ratio that increases beyond unity as a_m and t_r increase above unity (Fig. 6a and c). For any given combination of a_m and t_r, the stable cycle has a γ_ι/γ ratio that is almost constant (Fig. 6a).

For a given γ, the period of the stable population cycle increases almost linearly with an increase in a_m and t_r (Fig. 6d), with the period dependence on γ being somewhat elevated relative to the discrete model where $a_m = t_r = 1$ (Fig. 6b). Hence, for populations where γ is independent of a_m and t_r, we can expect an approximate linear relation between the population period T and life history periods like a_m and t_r. This implies a population cycle allometry, where T is expected to scales with the 1/4 and 1/6 power of body mass across species with intra-specific competition in two and three spatial dimensions (Witting 1995, 2017).

When only one parameter is altered at the time, the period is almost invariant of γ (Fig. 6f). This reflects that the decline in period with an increase in γ for dynamics with a given damping ratio, is counterbalanced by the increase in period that is caused by the increased stability of the cycle, as the γ_ι/γ ratio—that defines the damping ratio—declines with the increase in γ. For single parameter perturbations, the damping ratio is usually most strongly dependent on γ and γ_ι, showing only a small increase with t_r and a small decline with an increase in a_m (Fig. 6e).